Author Manuscript

Author Manuscript

Author Manuscript

Author Manuscript

HHS Public Access

Author manuscript

Anat Rec (Hoboken). Author manuscript; available in PMC 2016 May 01.

Published in final edited form as:

Anat Rec (Hoboken). 2015 May ; 298(5): 865–877. doi:10.1002/ar.23105.

BIOPSY PROVEN MEDULLARY SPONGE KIDNEY: Clinical findings, histopathology, and role of osteogenesis in stone and plaque formation

Andrew P. Evan[1], **Elaine M. Worcester**[2], **James C. Williams Jr.**[1], **Andre J. Sommer**[3], **James E. Lingeman**[4], **Carrie L. Phillips**[5], and **Fredric L. Coe**[2]

[1]Department of Anatomy and Cell Biology, Indiana University School of Medicine, Indianapolis, IN

[2]Nephrology Section, University of Chicago, Chicago, IL

[3]Department of Chemistry and Biochemistry, Miami University, Oxford, OH

[4]International Kidney Stone Institute, Methodist Hospital, Indianapolis, IN

[5]Department of Pathology, Indiana University Health, Indianapolis, IN

Abstract

Medullary sponge kidney (MSK) is associated with recurrent stone formation, but the clinical phenotype is unclear because patients with other disorders may be incorrectly labeled MSK. We studied 12 patients with histologic findings pathognomonic of MSK. All patients had an endoscopically recognizable pattern of papillary malformation, which may be segmental or diffuse. Affected papillae are enlarged and billowy, due to markedly enlarged inner medullary collecting ducts (IMCD), which contain small, mobile ductal stones. Patients had frequent dilation of Bellini ducts, with occasional mineral plugs. Stones may form over white (Randall's) plaque, but most renal pelvic stones are not attached, and have a similar morphology as ductal stones, which are a mixture of calcium oxalate and apatite. Patients had no abnormalities of urinary acidification or acid excretion; the most frequent metabolic abnormality was idiopathic hypercalciuria. Although both Runx2 and Osterix are expressed in papillae of MSK patients, no mineral deposition was seen at the sites of gene expression, arguing against a role of these genes in this process. Similar studies in idiopathic calcium stone formers showed no expression of these genes at sites of Randall's plaque. The most likely mechanism for stone formation in MSK appears to be crystallization due to urinary stasis in dilated IMCD with subsequent passage of ductal stones into the renal pelvis where they may serve as nuclei for stone formation.

Keywords

medullary sponge kidney; kidney stone; Randall's plaque; incomplete renal tubular acidosis; Runx2; Osterix

Corresponding Author: Andrew P. Evan, PhD, Department of Anatomy & Cell Biology, Indiana University School of Medicine, 635 Barnhill Drive, MS 5055, Indianapolis, IN 46220, aevan@iupui.edu, FAX: 317-278-2040.

No conflicts of interest financial or otherwise are declared by the authors.

Author Manuscript Author Manuscript Author Manuscript Author Manuscript

INTRODUCTION

Medullary sponge kidney (MSK) has traditionally been diagnosed by its characteristic radiographic appearance. Dilated terminal ducts of Bellini (BD) and inner medullary collecting ducts (IMCD), which often contain mineral deposits, produce a recognizable pattern best seen on intravenous pyelograms (Gambaro et al, 2013; Gambaro et al,, 2006): multiple papillary calcifications accompanied by a brushwork of dilated ducts that fill with contrast material. To date, almost all clinical and physiological studies of patients with MSK have relied upon radiographically diagnosed disease (Ginalski et al, 1990; O'Neill et al, 1981; Higashihara et al, 1984; Parks et al, 1982; McPhail et al, 2012; Morris et al, 1965; Harrison and Rose, 1979). But radiography, particularly in the absence of contrast, is inherently indirect as compared with inspection of tissues.

Modern surgical research techniques can in principle diagnose MSK more directly. Biopsy of papillae during surgery (Kuo et al, 2003) can document the well-known triad of undifferentiated interstitial cells, abnormal multilayered IMCD epithelium, and IMCD dilation which are the pathognomonic traits of this developmental abnormality (Darmady and Maclver, 1980; Ekstrom et al, 1959).

Having a group of biopsy-proven MSK patients should permit a clearer and more reliable clinical phenotype than one obtains from patients diagnosed by radiographic appearance: for example, types of stones formed, presence of tubule function defects such as renal tubular acidosis (RTA), and evidence of renal injury which is found in many forms of stone disease (Evan et al, 2014; Evan et al, 2010; Evan et al, 2007b; Evan et al, 2006). In addition, histologically defined cases permit a test of the hypothesis that stones and interstitial crystals in MSK might form via tissue osteogenesis as has been proposed by others (Mezzabotta et al, 2008; Gambaro et al, 2009).

We present here the first description of the intra-operative appearance, and clinical and laboratory characteristics of biopsy-proven MSK. In addition, we have measured expression of two key bone genes, Runx2 and Osterix, to test the osteogenic hypothesis.

As a control, and also because osteogenic mechanisms have been suggested as a mechanism for formation of white interstitial apatite (Randall's) plaque (Gambaro 2009; Gambaro 2004), we performed the same gene expression measurements in tissue sections from 9 previously published idiopathic calcium oxalate (CaOx) stone formers (ICSF).

MATERIALS AND METHODS

Subjects

Unlike our prior reports, our subjects were defined not by the type of stones formed, by clinical setting (such as ileostomy) or by underlying metabolic disorder (such as primary hyperparathyroidism). Instead, they represent all patients with the characteristic papillary characteristics of MSK who underwent papillary and cortical biopsy at the time of percutaneous nephrolithotomy (PNL) since the inception of the biopsy protocol in 1999. Patients may or may not have been labeled MSK prior to surgery, and some patients who

Author Manuscript Author Manuscript Author Manuscript Author Manuscript

were so labeled pre-operatively (usually based on the finding of nephrocalcinosis on radiographs) were not found to have the typical changes, and were removed from the MSK group.

MSK is a developmental abnormality of the kidney with three recognized anatomical traits by which it is distinguished from other related abnormalities. The hallmark of MSK is numerous dilated IMCD, which produce the spongy appearance for which the disease is named. Papillary interstitial cells have primitive characteristics which include a fibroblastic appearance (Darmady and Maclver, 1980; Ekstrom et al, 1959). Their numbers far exceed the normal cell density of human papillary interstitium. The epithelium is multi-layered in those IMCD, which are not cystic, while cystic dilated IMCD have single or multi-layered epithelium. All of our cases meet all three of these criteria.

We studied 12 MSK patients (Tables 1–3, **cases 1–12**) and also include previously unreported histopathologic data for 9 ICSF described in earlier publications (Evan et al, 2008; Evan et al, 2003). The study was approved by the Institutional Review Board Committee for Clarian Health Partners (#98-073).

Clinical laboratory studies

Clinical history was obtained directly, along with reviews of records. Radiographs were evaluated by us. Two 24-hour urine samples were collected while patients were on their usual diet and not taking medications that might alter stone risk factor measurements. Blood measurements were also drawn in the absence of treatments for stone disease. Measurements were as described elsewhere (Evan et al, 2014).

Controls

From a prior publication (Parks et al, 2009b) we extracted CaOx stone forming 'controls' for the present work, selecting those with complete data for urine NH4 and who also had stone analyses documenting lack of conversion from CaOx to >20% calcium phosphate (CaP) during our periods of observation. For each control we compiled the mean of three pre-treatment measurements to compare against the 24 pretreatment measurements from our 12 cases of MSK.

Biopsy protocol and plaque area determination

During PNL all accessible papillae were digitally imaged as described elsewhere for determination of white and yellow plaque area (Evan et al, 2014; Evan et al, 2007b). Yellow plaque was visible as elongated sites on the surface of the papilla. Biopsies were taken from the upper pole, inter-polar, and lower pole papillae and cortex when possible.

Tissue analysis

General—Twenty-one papillary and eight cortical biopsies were studied using light microscopy. All specimens were immersed in 5% paraformaldehyde in 0.1 mol/L phosphate buffer pH 7.4 (PPB).

Author Manuscript Author Manuscript Author Manuscript Author Manuscript

Light microscopy (Table 3)—Papillary and cortical specimens were prepared for histologic analysis as we have previously described (Evan et al, 2014). An additional set of cortical and papillary sections was cut at 7μ for infrared analysis as previously published (Evan et al, 2007a). All paraffin sections were imaged with a Leica DMR photomicroscope with RT Slider Spot camera equipped with fluorescent filters for DAPI, FITC, Rhodamine and a triple filter for all three.

In a double blind design, a renal pathologist (CP) performed a semi-quantitative analysis (Evan et al, 2014) using the Jones' silver stained and PAS stained cortical sections from all patients except patients 1, 3 and 5, from whom no tissue was available.

Runx2 and osterix staining—Runx2 and osterix immunohistochemistry was performed according to the peroxidase-antiperoxidase (PAP) method as we reported in our previous study (Evan et al, 2008). The paraffin slides were deparaffinized and rehydrated through graded alcohols and blocked for nonspecific protein binding using 20% normal goat serum in 0.1 mol/L phosphate-buffered saline (PBS) at room temperature for 2 hours. A recombinant human Runx2/CBFA1 primary antibody derived from a rat monoclonal IgG2B clone was purchased from R and D Systems (Minneapolis, MN) and used at a 1:25 dilution. A human Osterix primary antibody was purchased from Santa Cruz Biotechnology, Inc (Dallas, TX) and used at a 1:35 dilution. The secondary antibody was biotinylated goat anti-mouse IgG (Sigma, St. Louis, MO). Reactivity was detected with the ELITE ABC kit (Vector Labs, Burlingame, CA) and DAB (3,3-diaminobenzidine tetrahydrochloride). DAB in Tris-HCl buffer was used as the chromogen. All sections were covered with DAB solution (0.05 mol/L Tris-HCl, 0.001% hydrogen peroxide, and 0.10% DAB), and incubated for approximately 10 minutes. Finally, each slide was rinsed well with buffer and lightly counterstained with hematoxylin. Controls were performed with the elimination of the primary antibody and showed no staining.

Crystal deposits and stones

Infrared—Attenuated Total Internal Reflection (ATR) Fourier Transform Infrared Microspectroscopy (μ-FTIR) was used as described elsewhere (Anderson et al, 2005) to identify mineral types in crystal deposits in cortical and papillary biopsies.

μCT—All papillary biopsies underwent μCT analysis with the SkyScan-1072 (Vluchtenburgstraat 3, B-2630 Aartselaar, Belgium) high-resolution desktop μCT system as previously described (Williams et al, 2010).

A second mCT system, the Scanco mCT 20 instrument (Scanco Medical AG, Bassersdorf, Switzerland), was used to determine mineral composition of the crystalline deposits in papillary biopsies analyzed by the SkyScan mCT device and stones as we have previously published. Mineral type was determined by x-ray attenuation values, as previously described (Zarse et al, 2004).

Some pelvic and intraductal stones collected by our team at the time of stone removal were sent to a clinical laboratory for analysis of mineral composition. The rest of the stones collected were analyzed by μCT, as described above for biopsies. Typical stone scans were

Author Manuscript Author Manuscript Author Manuscript Author Manuscript

completed at 60 kV and reconstructed to create 3D image stacks with cubic voxels 2–20 μm on a side, depending on the total size of the stone. Stone mineral was identified by a combination of x-ray attenuation values and visible morphology. Selected specimens were additionally analyzed using infrared spectroscopy (Bruker Alpha-T Spectrometer) using the KBr pellet method, for confirmation of mineral type (Williams et al, 2010).

RESULTS

Clinical and laboratory findings

Patients—We studied 12 patients with MSK proven by intra-operative papillary biopsy. The patients (4 male) were characterized by frequent stone episodes, as well as frequent urinary tract infections (Table 1). Stone analyses in Table 1 are only those obtained from patient charts and provided for patient care from a variety of commercial laboratories. More detailed analyses of stones removed during surgery were obtained from our research laboratory (below).

Radiological findings—Papillary calcification was present in all patients (Fig. 1, **panel a**). As deposits became extensive, some reached the cortico-medullary junction and even the renal capsule (Fig. 1, **panels a and b**). Without contrast, there is nothing about the radiographic pattern unique to MSK (Fig. 1, **compare panel a to panels c – e**).

Blood and urine measurements—Serum chemistries were generally normal, without evidence for hypokalemia or reduced bicarbonate level (Table 2). Hypercalciuria was present in 8 patients (Table 2) using the cut point of 140 mg/gm creatinine that is applicable to both sexes. Other common stone risk factors were not found apart from low urine citrate in 4 cases (cases 1, 3, 4, and 9), and substantial urine oxalate excretion in 3 cases (cases 1, 3, and 11).

Urine pH, ammonia, and titratable acidity of the MSK patients did not differ from a group of previously reported CaOx stone forming controls **(METHODS)**. In addition, there was no interaction between subject type (MSK vs. CaOx controls) and the relationship between urine ammonia and urine pH (detailed results not shown). In other words, there was no evidence of abnormally high urine ammonia in relation to pH as has been described in incomplete RTA.

Surgical Observations

Papillary morphology unique to MSK—Of our 12 cases, 4 had only unilateral PNL (Table 1, **cases 2–5**). Of these 4, 2 had unilateral stones and 2 had bilateral stones but only one side was treated (Table 1, **cases 3 and 4**). In all cases, the involved papillae were generally rounded and enlarged with a billowy appearance we have not encountered in other types of stone formers; compare Figure 2, **panels a and b**, to Figure 2, **panel e**. As part of the general rounding of contours, the papillary tips were blunted (Fig. 2 **panels a and b**). These changes of MSK were diffuse - involved all papillae of the same kidney - with the exceptions of cases 4, 5, 10, and 12. In case 10, both kidneys were observed and each had segmental disease: some papillae were normal in appearance (Fig. 2, **panels d and e**). In

Author Manuscript Author Manuscript Author Manuscript Author Manuscript

cases 4 and 5, disease was segmental in the one kidney in each case that was studied. In case 12, one kidney had segmental involvement and the other universal involvement. Because of their abnormal endoscopic appearances, a surgeon can reliably distinguish MSK - involved papillae from normal papillae in patients with segmental disease.

Mineral deposition and stone formation common to MSK and other diseases—Although surgical observations and mapping were performed on all patients, harvesting of stones and plugs could not be accomplished in cases 3, 4, and 5 for clinical reasons; therefore these three patients are not included in Table 3. Dilated Bellini ducts (BD) were frequent; all of the MSK-involved papillae had at least one and many had numerous dilated BD. Despite the number of dilated ducts, only 6 ducts in 2 patients (Table 3, **patients 7 and 8**) had protruding mineral plugs (Fig. 2, **panel c**; Table 3). Yellow elongate deposits on the papillary surface that reflect IMCD deposits were also scanty (Fig. 2, **panel a**, and Table 4). In the papillae without changes of MSK (**cases 4, 5, 10, and 12**) we found no dilated BD (Fig. 2, **panels d and e**), and no plugs nor yellow elongate deposits.

There were scattered areas of white (Randall's) plaque in all 12 patients (Fig. 2, **panels a, d and e**, Table 4). In three patients (Table 3, **patients 1, 10, and 11**) we found stones growing attached to white plaque (Figure 2, **panel d**). Some stones were free in the renal pelvis or renal calyces (Figure 2, **panel b** and Table 3) and we could not determine their origins.

IMCD ductal stones—Ductal stones were observed in all of the MSK-involved papillae of our patients (Fig. 3, **panel a**). They appeared as yellow sub-urothelial stones rather than as dark shadows as observed in cystinuria. When these ducts were unroofed using the holmium laser, numerous ductal stones (Fig. 3, **panels b and c**) were present. Unlike plugs in BD or IMCD, which are held firmly in place, the stones in the dilated IMCD and BD were unattached, and rolled out after unroofing like marbles on a tabletop. Viewed from above, the unroofed dilated ducts of the MSK patients appear as elaborate honeycomb labyrinths unlike anything we have seen before in stone formers (Fig. 3, **panel d**). It is specifically the volume of the massively dilated stone-filled ducts that produces the odd shape of the MSK papillae.

Fine structure of IMCD ductal stones, BD plugs and their overgrowths, stones growing on white plaque, and renal pelvic stones

IMCD ductal stones—We were able to harvest ductal stones from 7 of the 12 patients (Table 3). Using high resolution CT, ductal stones revealed alternating laminar deposits of hydroxyapatite (HA) and CaOx. H_2O (COM) with layers of organic materials (Fig. 4, **panels a and b**). In one patient, brushite was also present.

BD plugs and their overgrowths—We found BD plugs in only 2 patients (Table 3). The 6 BD plugs (Fig. 4 **panels c and d**) were also a mixture of COM and HA (**composition in** Table 3). Viewed along their long axes (Fig. 4, **panels c and d**) the intra-ductal material of BD plugs from patient 7 was mostly HA (Table 3), whereas the ductal material from patient 8 was 60% CaOx, the rest being HA. Viewed in cross section (Fig. 4, **panels e and f**) the body of a plug that was within the BD of patient 7 reveals a ring like concentric pattern

Author Manuscript Author Manuscript Author Manuscript Author Manuscript

of HA, the laminae being apatite of greater and lesser x ray density. When viewed in cross section, the overgrowth on the plug (Fig. 4, **panel g**) contained concentric laminae of alternating HA and COM; this was true in both patients (Table 3).

Stones growing on white plaque—One stone each from patients 1 and 10 formed on white plaque and were removed. That from patient 1 (Table 3) was mainly CaOx. That from patient 10 was lost to analysis. Two stones from patient 11 were attached to white plaque. Each displayed the typical HA attachment site of stones that have grown over white plaque. Both contained brushite, CaOx and HA (mean values for both are in Table 3).

Renal pelvic stones—Many stones appeared free in the pelvis (Table 3) and did not display the typical HA attachment site of stones that have grown on white plaque. These ranged from mainly CaOx (a few with traces of uric acid) to mainly HA and brushite. Although calyces contained free stones, none were harvested for analysis. Alternating laminae of CaOx and matrix or HA, and lamina of HA of varying density were found as in the ductal stones.

Histopathology

Papillum—We found ductal stones only in the dilated IMCD (Fig. 5, **panels a, c, and d**). Ductal stones stained with Yasue, which is compatible with either CAP or CaOx. Polarizing optics revealed a mixture of birefringent and non birefringent crystals (Fig. 5, **panel d**). By micro-FTIR the crystals were a mixture of COM and HA (**not shown**) consistent with the high-resolution CT findings already presented (Table 3). Of note, stones were not attached to the IMCD epithelial cells, which were uninjured in appearance. Frequent cystic IMCD were without stones, meaning the dilation can precede stones (Fig. 5, **panels a and c**).

Large regions of interstitium (Fig. 5, **panels a to c**) contained numbers of primitive interstitial cells. In regions surrounding even the most extensively stone filled IMCD, we found no evidence for interstitial fibrosis (Fig. 5, **panels a–c**). We visualized only one IMCD plug (Fig. 5, **panel a**). Unlike our usual experience this plugged IMCD was not surrounded by interstitial reaction nor were the epithelial cells damaged in appearance. However, the epithelium was abnormal in being multilayered, as is the rule in MSK. By FTIR, the plug was HA (not shown). We did not obtain any biopsy sections for histopathology that contained BD crystal plugs, so we cannot comment on whether such plugs produce local peri-ductal interstitial fibrosis.

Despite many tubules containing ductal stones, no papillae were flattened or deformed apart from the plumpness we already mentioned. White plaque abundance exceeded the normal upper limit of 1% in 6 of 12 patients (Table 4) but was generally below the high levels common in ICSF of 8% or more. Yellow plaque was very sparse, as expected given the paucity of IMCD plugs.

The density of intra-tubular mineral (deposits plus ductal stones) determined by micro CT of biopsy tissue varied from 1 to 14 deposits per cubic mm (Table 4). A majority of deposits were ductal stones (Table 4).

Author Manuscript Author Manuscript Author Manuscript Author Manuscript

Cortex—In general the cortex was normal or near normal in our patients (Table 4). Glomerular obsolescence, tubular atrophy, and interstitial fibrosis are about the same as in otherwise unselected people of similar age (**not illustrated in figures**). In patients 4 and 10, however, changes were above those expected in otherwise normal people.

Expression of bone genes by interstitial cells of patients with MSK and ICSF

Runx2—In papillary tissue from 10 of the 12 MSK patients, staining was positive in the interstitial cells but not tubular epithelial cells (Fig. 6, **panels a – c; cases 3 and 4 were not studied**). In 36 tissue samples from 9 ICSF (4 samples for each patient), we found no evidence for Runx2 expression in papillary tissue even though every section contained at least some Randall's plaque (Fig. 6, **panel d**).

Osterix—In tissue from the same 10 MSK patients staining was positive and localized to the interstitial cells (Fig. 7, **panels a–c, MSK patients 2, 3, 1, respectively**). As for Runx2, staining was negative in tissues from the 36 samples from 9 ICSF (Fig. 7, **panel d**).

Evidence for mineral formation at sites of bone gene expression

We tested for the presence of mineral formation at sites of bone gene expression in all 10 MSK cases in which we performed immunostaining. To detect interstitial mineral, we stained MSK tissues with Yasue. In 34 areas positive for bone gene expression, we found mineral stain only once (X^2=31, $p<0.001$). We found no bone gene expression in IMCD of MSK despite the formation of stones and deposits in that tubule segment. This means that osteogenesis cannot be a cause of stone formation at these sites. In none of the 36 sections from ICSF did we find bone gene expression although we did find abundant interstitial apatite plaque.

DISCUSSION

Diagnosis

Our cases are defined by multilayered hyperplastic epithelia in undilated IMCD, single layered epithelia in dilated IMCD, and primitive interstitial cells that resemble embryonic cells (Darmady and Maclver, 1980; Ekstrom et al, 1959). Ekstrom et al (1959) documented these MSK pathognomonic histologic changes by examining nephrectomy obtained kidneys from 15 patients who were diagnosed with MSK using urography. Since 12 cases here have all three findings, they are authentic MSK.

Distinct and unique surgical anatomy permits precise diagnosis

The characteristic shape of papillae involved with MSK permits differentiation from all other types of stone disease: rounded contours, enlargement, and a puffy, inflated, soft and billowy appearance. That this surgical appearance is diagnostic of MSK, whether diffuse or segmental supports the idea that clinical diagnosis of MSK must rely on direct visualization at the time of surgery, or perhaps intravenous pyelography or CT urography (Koraishy et al, 2014; Maw et al, 2007), but not on other forms of radiography.

Author Manuscript Author Manuscript Author Manuscript Author Manuscript

Kidney disease is minimal

Apart from kidney stones, MSK seems benign. Papillary interstitial fibrosis is absent despite IMCD ductal stones. We did not obtain biopsy tissue that included BD plugs, so we do not know if interstitial fibrosis surrounded them as is the case in other diseases with such plugs (Evan et al, 2014; Coe et al, 2010). Many dilated IMCD were without stones (Fabris et al, 2013; Elkin and Bernstein, 1969; Kendall et al, 1974). The cortices of our patients were generally normal as in ICSF (Evan et al, 2014). Although urinary tract infections were common, none progressed to pyelonephritis as others have (Morris et al, 1965; Parks et al, 1982; Chu et al, 2009) we did not observe this.

Incomplete RTA (Wrong and Davies, 1959) was absent. Ammonia excretion was normal, and only 4 of our 12 patients were hypocitraturic. An abnormal response to acid load has been described in up to 40% of MSK patients (Higashihara et al, 1984; Morris et al, 1965; Osther et al, 1994); we did not perform this test. Idiopathic hypercalciuria was the stone risk factor most frequently present, as has been reported by others (O'Neill et al, 1981; McPhail et al, 2012; Fabris et al, 2013).

Seven kinds of renal mineralization are present in MSK

We shall call stones patients pass or have removed 'clinical stones' for clarity. We also identified: ductal stones; BD plugs; plug overgrowths; IMCD plugs; stones growing on interstitial white apatite plaque; and renal pelvic stones. In all but two of our present cases, the composition of these mineralizations from a given patient tend to match (Table 5) suggesting that crystallization is being controlled by a reasonably uniform set of forces. Clinical stones, which must be derived from one or more of these intrarenal sources. Stones in our MSK patients contained roughly equivalent amounts of CaOx and CaP (as HA and occasionally brushite), and even traces of uric acid in stones (Harrison and Rose, 1979; McPhail et al, 2012).

Ductal stones—All of our patients formed numerous, tiny, stones in dilated IMCD (Table 5). They differ from IMCD and BD plugs, which take the elongate shape of their enclosure and adhere to the tubule lining, by rolling freely within their ducts and being round like marbles. Whereas IMCD and BD plugs destroy tubule epithelia and ultimately find their way to the basement membranes (Evan et al, 2014; Coe et al, 2010), ductal stones do not adhere to or damage epithelia.

Like all supersaturated solutions, urine forms crystals over time. Simple retention within cystic IMCD may allows stagnant urine to create nuclei and eventually tiny stones. The numerous urine molecules that delay nucleation, growth, cell attachment, and aggregation of crystals (Worcester, 1994; Wesson et al, 1998) may coat the stones minimizing attachment to epithelia (Kumar et al, 2003). Both of these assertions are by way of hypotheses for future experiments to test.

BD plugs and overgrowths—Only 2 patients formed BD plugs, all of which had overgrowths (Tables 3 and 5). Being so few, their clinical significance is unclear.

Author Manuscript Author Manuscript Author Manuscript Author Manuscript

IMCD plugs—The one we visualized histopathologically produced no interstitial reaction or tubule epithelial damage (Evan et al, 2014). By contrast, in all of our other stone phenotypes (Coe et al, 2010) IMCD plugs cause both interstitial and epithelial injury and inflammation. Perhaps, being an abnormal epithelium, the MSK cells may react to crystals differently than normal epithelia. Of note, the plug was pure HA by FTIR, differing from all other mineralizations in that patient (Table 1, **case 1**).

Stones growing on white plaque—These stones did not differ from those we have described before (Miller et al, 2009; Evan et al, 2003). In one patient (**Patient 11**) the stones were odd in containing brushite, CaOx and HA; the HA attachment site was evident.

Why pelvic and clinical stones form—Growth on white plaque seems too slight to account for clinical and pelvic stone formation. Likewise, BD plugs and their overgrowths were also scarce. This leaves ductal stones as a possible source for stone disease. Perhaps they exit their ducts and grow into clinically important stones: they are nucleating centers created by stasis in dilated IMCD. The similar fine structure morphology of ductal stones and renal pelvic stones is consistent with this hypothesis.

Also consistent with it is the urine chemistry. Although CaOx and CaP SS were high in some patients (Table 2) mean values in MSK patients are not different from those we have found in normal subjects and are below those of ICSF (Parks et al, 2009a). Therefore high SS itself does not seem as reasonable a main mechanism for crystal deposits in MSK as in other forms of stone disease. The relative lack of metabolic risk factors for stone formation in patients with MSK has also been noted by others (Ginalski et al, 1990).

A future test of the ductal stone nucleation hypothesis would be to ask if calyceal stones were indeed mainly found in association with MSK papillae and calyces with normal papillae mainly free of stones. This test would require a level of detail and a case series beyond what is available here.

Osteogenesis is not a mechanism for stones in MSK or for white plaque in ICSF

Our findings falsify the hypothesis that tissue osteogenesis creates ductal stones or interstitial plaque because it requires that key bone genes be expressed at sites of mineral formation (Mezzabotta et al, 2008; Gambaro et al, 2009). We found expression of Runx2 and Osterix in papillary interstitial cells of MSK but conclusively excluded mineral formation at sites of their expression. Bone genes were not expressed in regions of interstitial plaque of the MSK patients our in 36 tissue sections of 9 ICSF. Our failure to confirm two necessary predictions of the tissue osteogenesis hypothesis falsifies it in these two specific kinds of patients.

Conclusions

Given the uniform and distinctive appearance of MSK during surgery it is now possible to diagnose MSK with virtual certainty via intraoperative digital endoscopy. Papillae have a billowy appearance; IMCD ductal stones floating freely are visible through the urothelium. On de-roofing such IMCD, one finds numerous free-floating ductal stones and on biopsy a

Author Manuscript Author Manuscript Author Manuscript Author Manuscript

cystic IMCD morphology. Dilated IMCD are not cystic in any disease but MSK. Papillary biopsy is definitive but probably not practical or necessary for clinical diagnosis. However attractive, the osteogenic hypothesis fails to explain either mineralization in MSK or plaque formation in ICSF. A likely mechanism for clinical stones in MSK is that ductal stones form via stasis, exit calyces, and act as nucleating sites in the renal pelvis.

ACKNOWLEDGEMENTS

This work was supported by National Institute of Diabetes and Digestive and Kidney Diseases grant PO1-DK-56788.

Literature Cited

Anderson J, Dellomo J, Sommer A, Evan A, Bledsoe S. A concerted protocol for the analysis of mineral deposits in biopsied tissue using infrared microanalysis. Urol Res. 2005; 33:213–219. [PubMed: 15703966]

Carboni I, Andreucci E, Caruso MR, Ciccone R, Zuffardi O, Genuardi M, Pela I, Giglio S. Medullary sponge kidney associated with primary distal renal tubular acidosis and mutations of the H+ATPase genes. Nephrol Dial Transplant. 2009; 24:2734–2738. [PubMed: 19364879]

Chu HY, Yan MT, Lin SH. Recurrent pyelonephritis as a sign of 'sponge kidney'. Cleve Clin J Med. 2009; 76:479–480. [PubMed: 19652042]

Coe FL, Evan AP, Lingeman JE, Worcester EM. Plaque and deposits in nine human stone diseases. Urol Res. 2010; 38:239–247. [PubMed: 20625890]

Darmady, EM.; MacIver, AG. Renal cystic disease. In: Crowford, T., editor. Renal Pathology. London: Butterworth and Co.; 1980. p. 93-121.

Donnelly S, Kamel KS, Vasuvattakul S, Narins RG, Halperin ML. Might distal renal tubular acidosis be a proximal tubular cell disorder? Am J Kidney Dis. 1992; 19:272–281. [PubMed: 1553972]

Ekstrom, T.; Engfeldt, B.; Lagergren, C.; Lindvall, N. Medullary sponge kidney: a roentgenologic, clinical, histopathological and biophysical study. Stockholm: Almquist and Wiksell; 1959.

Elkin M, Bernstein J. Cystic diseases of the kidney--radiological and pathological considerations. Clin Radiol. 1969; 20:65–82. [PubMed: 5774094]

Evan AP, Lingeman JE, Coe FL, Parks JH, Bledsoe SB, Shao Y, Sommer AJ, Paterson RF, Kuo RL, Grynpas M. Randall's plaque of patients with nephrolithiasis begins in basement membranes of thin loops of Henle. J Clin Invest. 2003; 111:607–616. [PubMed: 12618515]

Evan AP, Coe FL, Lingeman JE, Shao Y, Matlaga BR, Kim SC, Bledsoe SB, Sommer AJ, Grynpas M, Phillips CL, Worcester EM. Renal crystal deposits and histopathology in patients with cystine stones. Kidney Int. 2006; 69:2227–2235. [PubMed: 16710357]

Evan AP, Coe FL, Lingeman JE, Shao Y, Sommer AJ, Bledsoe SB, Anderson JC, Worcester EM. Mechanism of formation of human calcium oxalate renal stones on Randall's plaque. Anat Rec (Hoboken). 2007a; 290:1315–1323. [PubMed: 17724713]

Evan AP, Lingeman J, Coe F, Shao Y, Miller N, Matlaga B, Phillips C, Sommer A, Worcester E. Renal histopathology of stone-forming patients with distal renal tubular acidosis. Kidney Int. 2007b; 71:795–801. [PubMed: 17264873]

Evan AP, Coe FL, Gillen D, Lingeman JE, Bledsoe S, Worcester EM. Renal intratubular crystals and hyaluronan staining occur in stone formers with bypass surgery but not with idiopathic calcium oxalate stones. Anat Rec (Hoboken). 2008; 291:325–334. [PubMed: 18286613]

Evan AP, Lingeman JE, Worcester EM, Bledsoe SB, Sommer AJ, Williams JC Jr, Krambeck AE, Philips CL, Coe FL. Renal histopathology and crystal deposits in patients with small bowel resection and calcium oxalate stone disease. Kidney Int. 2010; 78:310–317. [PubMed: 20428098]

Evan AP, Lingeman JE, Worcester EM, Sommer AJ, Phillips CL, Williams JC, Coe FL. Contrasting Histopathology and Crystal Deposits in Kidneys of Idiopathic Stone Formers Who Produce Hydroxy Apatite, Brushite, or Calcium Oxalate Stones. Anat Rec (Hoboken). 2014 epub.

Author Manuscript Author Manuscript Author Manuscript Author Manuscript

Fabris A, Lupo A, Bernich P, Abaterusso C, Marchionna N, Nouvenne A, Gambaro G. Long-term treatment with potassium citrate and renal stones in medullary sponge kidney. Clin J Am Soc Nephrol. 2010; 5:1663–1668. [PubMed: 20576821]

Fabris A, Anglani F, Lupo A, Gambaro G. Medullary sponge kidney: state of the art. Nephrol Dial Transplant. 2013; 28:1111–1119. [PubMed: 23229933]

Gambaro G, D'Angelo A, Fabris A, Tosetto E, Anglani F, Lupo A. Crystals, Randall's plaques and renal stones: do bone and atherosclerosis teach us something? J Nephrol. 2004; 17:774–777. [PubMed: 15593050]

Gambaro G, Feltrin GP, Lupo A, Bonfante L, D'Angelo A, Antonello A. Medullary sponge kidney (Lenarduzzi-Cacchi-Ricci disease): a Padua Medical School discovery in the 1930s. Kidney Int. 2006; 69:663–670. [PubMed: 16395272]

Gambaro G, Abaterusso C, Fabris A, Ruggera L, Zattoni F, Del PD, D'Angelo A, Anglani F. The origin of nephrocalcinosis, Randall's plaque and renal stones: a cell biology viewpoint. Arch Ital Urol Androl. 2009; 81:166–170. [PubMed: 19911679]

Gambaro G, Danza FM, Fabris A. Medullary sponge kidney. Curr Opin Nephrol Hypertens. 2013; 22:421–426. [PubMed: 23680648]

Ginalski JM, Portmann L, Jaeger P. Does medullary sponge kidney cause nephrolithiasis? AJR Am J Roentgenol. 1990; 155:299–302. [PubMed: 2115256]

Harrison AR, Rose GA. Medullary sponge kidney. Urol Res. 1979; 7:197–207. [PubMed: 505682]

Higashihara E, Nutahara K, Tago K, Ueno A, Niijima T. Medullary sponge kidney and renal acidification defect. Kidney Int. 1984; 25:453–459. [PubMed: 6727141]

Kendall AR, Pollack HM, Karafin L. Congenital cystic disease of kidney: classification and manifestations. Urology. 1974; 4:635–642. [PubMed: 4616433]

Koraishy FM, Ngo TT, Israel GM, Dahl NK. CT Urography for the Diagnosis of Medullary Sponge Kidney. Am J Nephrol. 2014; 39:165–170. [PubMed: 24531190]

Kumar V, Farell G, Lieske JC. Whole urinary proteins coat calcium oxalate monohydrate crystals to greatly decrease their adhesion to renal cells. J Urol. 2003; 170:221–225. [PubMed: 12796693]

Kuo RL, Lingeman JE, Evan AP, Paterson RF, Bledsoe SB, Kim SC, Munch LC, Coe FL. Endoscopic renal papillary biopsies: a tissue retrieval technique for histological studies in patients with nephrolithiasis. J Urol. 2003; 170:2186–2189. [PubMed: 14634375]

Maw AM, Megibow AJ, Grasso M, Goldfarb DS. Diagnosis of medullary sponge kidney by computed tomographic urography. Am J Kidney Dis. 2007; 50:146–150. [PubMed: 17591535]

McPhail EF, Gettman MT, Patterson DE, Rangel LJ, Krambeck AE. Nephrolithiasis in medullary sponge kidney: evaluation of clinical and metabolic features. Urology. 2012; 79:277–281. [PubMed: 22014971]

Mezzabotta F, Ceol M, Torregrossa R, Del Prete D, Tiralongo E, Fabris A, Della Vella M, D'Angelo A, Gambaro G, Anglani F. Spontaneous calcification process in a primary culture of renal cells from a patient with MSK carrying a GDNF mutation. J Am Soc Nephrol. 2008; 19:75A.

Miller NL, Gillen DL, Williams JC Jr, Evan AP, Bledsoe SB, Coe FL, Worcester EM, Matlaga BR, Munch LC, Lingeman JE. A formal test of the hypothesis that idiopathic calcium oxalate stones grow on Randall's plaque. BJU Int. 2009; 103:966–971. [PubMed: 19021625]

Miller NL, Humphreys MR, Coe FL, Evan AP, Bledsoe SB, Handa SE, Lingeman JE. Nephrocalcinosis: re-defined in the era of endourology. Urol Res. 2010; 38:421–427. [PubMed: 21057942]

Morris RC, Yamauchi H, Palubinskas AJ, Howenstine J. Medullary Sponge Kidney. Am J Med. 1965; 38:883–892. [PubMed: 14310004]

O'Neill M, Breslau NA, Pak CY. Metabolic evaluation of nephrolithiasis in patients with medullary sponge kidney. JAMA. 1981; 245:1233–1236. [PubMed: 7206112]

Osther PJ, Mathiasen H, Hansen AB, Nissen HM. Urinary acidification and urinary excretion of calcium and citrate in women with bilateral medullary sponge kidney. Urol Int. 1994; 52:126–130. [PubMed: 8203049]

Parks JH, Coe FL, Strauss AL. Calcium nephrolithiasis and medullary sponge kidney in women. N Engl J Med. 1982; 306:1088–1091. [PubMed: 7070404]

Author Manuscript Author Manuscript Author Manuscript Author Manuscript

Parks JH, Coe FL, Evan AP, Worcester EM. Clinical and laboratory characteristics of calcium stone-formers with and without primary hyperparathyroidism. BJU Int. 2009a; 103:670–678. [PubMed: 18793297]

Parks JH, Coe FL, Evan AP, Worcester EM. Urine pH in renal calcium stone formers who do and do not increase stone phosphate content with time. Nephrol Dial Transplant. 2009b; 24:130–136. [PubMed: 18662977]

Wesson JA, Worcester EM, Wiessner JH, Mandel NS, Kleinman JG. Control of calcium oxalate crystal structure and cell adherence by urinary macromolecules. Kidney Int. 1998; 53:952–957. [PubMed: 9551403]

Williams JC Jr, McAteer JA, Evan AP, Lingeman JE. Micro-computed tomography for analysis of urinary calculi. Urol Res. 2010; 38:477–484. [PubMed: 20967434]

Worcester E. Urinary calcium oxalate crystal growth inhibitors. J Am Soc Nephrol. 1994; 5:S46–S53. [PubMed: 7873744]

Wrong O, Davies HE. The excretion of acid in renal disease. Q J Med. 1959; 28:259–313. [PubMed: 13658353]

Yagisawa T, Kobayashi C, Hayashi T, Yoshida A, Toma H. Contributory metabolic factors in the development of nephrolithiasis in patients with medullary sponge kidney. Am J Kidney Dis. 2001; 37:1140–1143. [PubMed: 11382681]

Zarse CA, McAteer JA, Tann M, Sommer AJ, Kim SC, Paterson RF, Hatt EK, Lingeman JE, Evan AP, Williams JC Jr. Nondestructive analysis of urinary calculi using micro computed tomography. BMC Urol. 2004; 13:15. [PubMed: 15596006]

Author Manuscript Author Manuscript Author Manuscript Author Manuscript

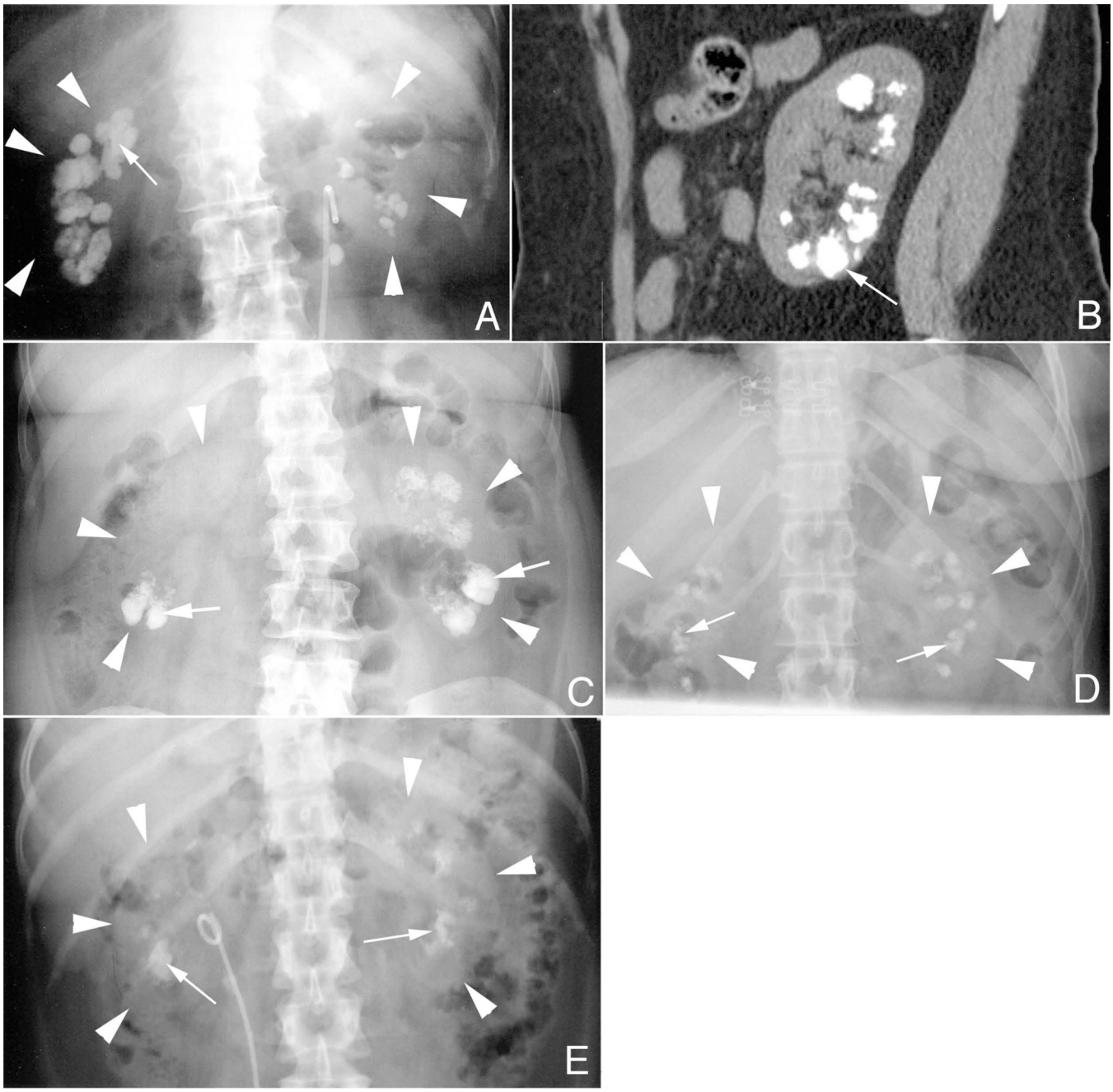

Figure 1. Radiological findings in MSK stone formers

Panel a is a KUB from MSK patient 8 showing bilateral renal calcifications (arrow). The renal capsules of both the right and left kidneys are outlined by white arrowheads in panels a–d. By CT (panel b) some deposits (arrow) are seen extending from the cortico-medullary junction to the renal capsule. This pattern of deposits (arrows) is also seen in patients with primary hyperparathyroidism (panel c), idiopathic calcium phosphate stone disease (panel d), and distal renal tubular acidosis (panel e).

Author Manuscript Author Manuscript Author Manuscript Author Manuscript

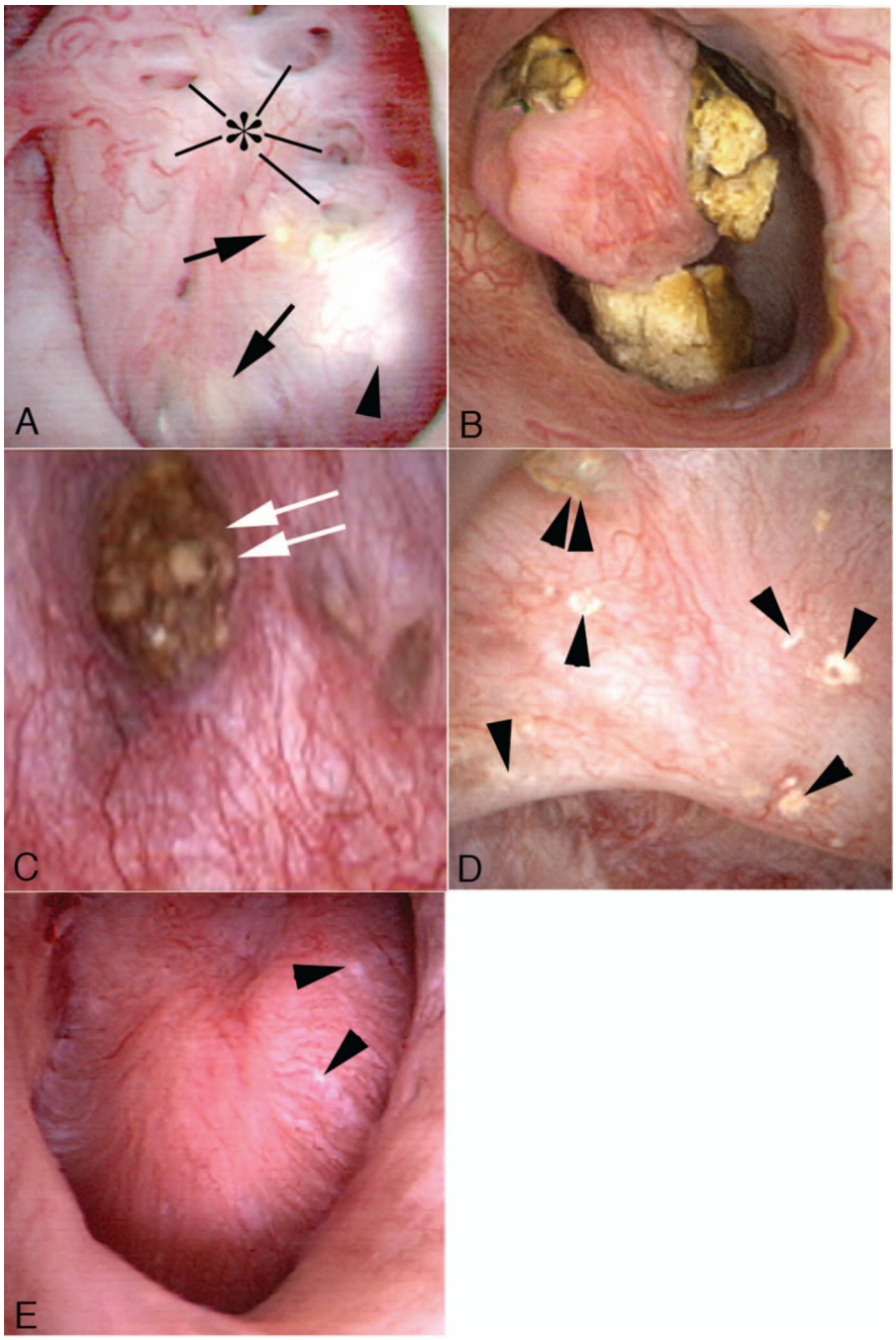

Figure 2. Endoscopic images of renal papilla from MSK stone formers

The affected papillae are characterized by a rounding of contours and enlargement, which creates a billowy appearance (panels a and b). As part of the general rounding of contours, the papillary tips are blunted. These papillae also show sites of white (panel a, arrowhead) and yellow (panel a, arrows) plaque, and dilated opening of ducts of Bellini with (panel c, double arrow) and without deposits (panel a, asterisk). An occasional calyceal stone is noted (panel c). The unaffected papillae possess a normal morphology as seen in the compound papillum in panel d and single papillum in panel e (case 5); note numerous sites of white

plaque (arrowheads) and an attached stone (double arrowhead). The unique morphology of affected papillae of MSK patients can be characteristic of all papillae (diffuse pattern) of a kidney or only some of the papillae (segmental pattern).

Author Manuscript Author Manuscript Author Manuscript Author Manuscript

Author Manuscript Author Manuscript Author Manuscript Author Manuscript

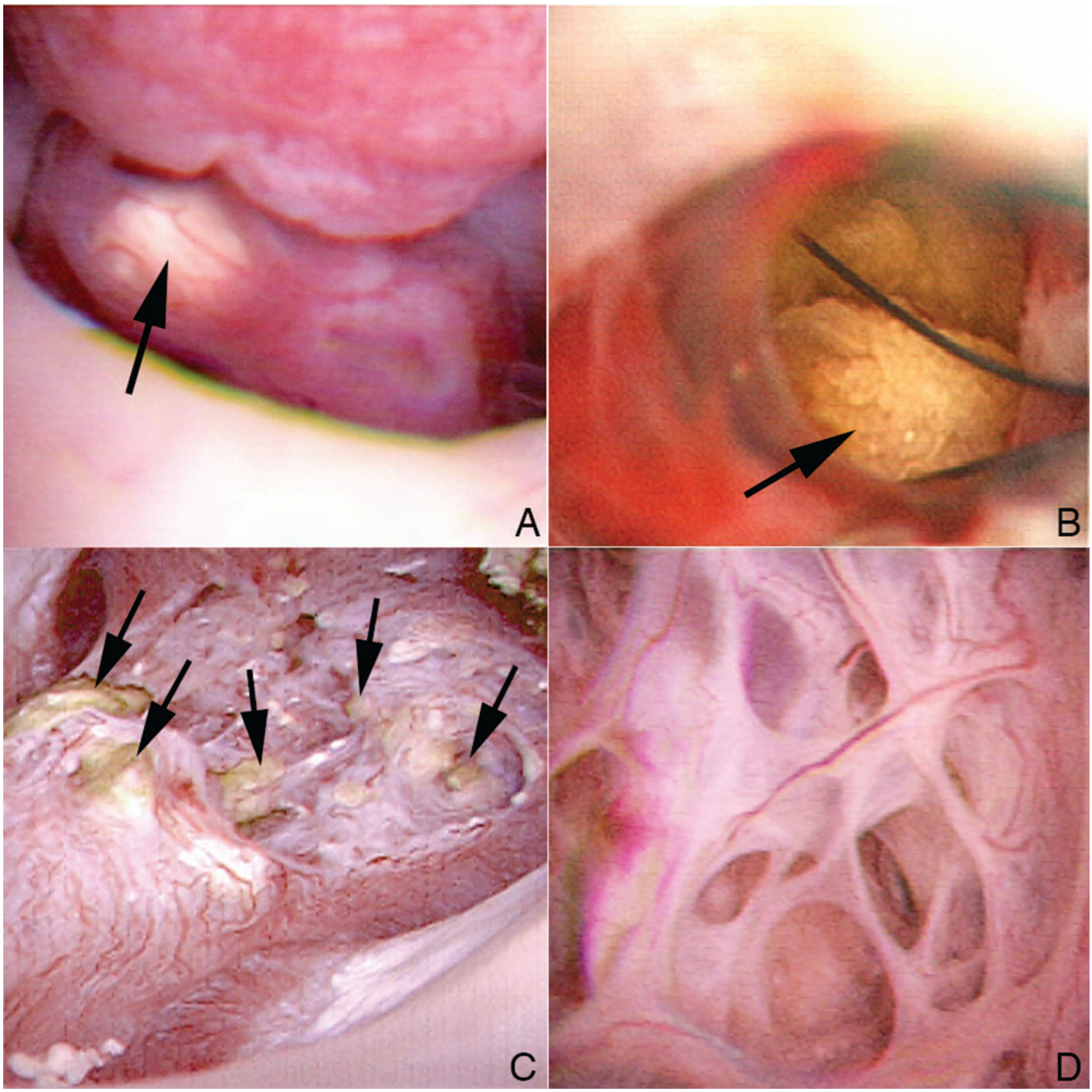

Figure 3. Appearance of intact and unroofed IMCD containing ductal stones

Ductal stones were observed in the billowy MSK papillae as yellow sub-urothelial deposits (panel a, arrow). When the thin urothelial lining that covers these ductal stones is unroofed using the holmium laser (panel b), the unattached stones (arrow) roll out like marbles on a tabletop. When all of the dilated IMCD from a particular papillum are unroofed to release their intra-ductal stones (panel c, arrows), a massive honeycomb labyrinth like pattern of the papillum (panel d) is seen.

Author Manuscript Author Manuscript Author Manuscript Author Manuscript

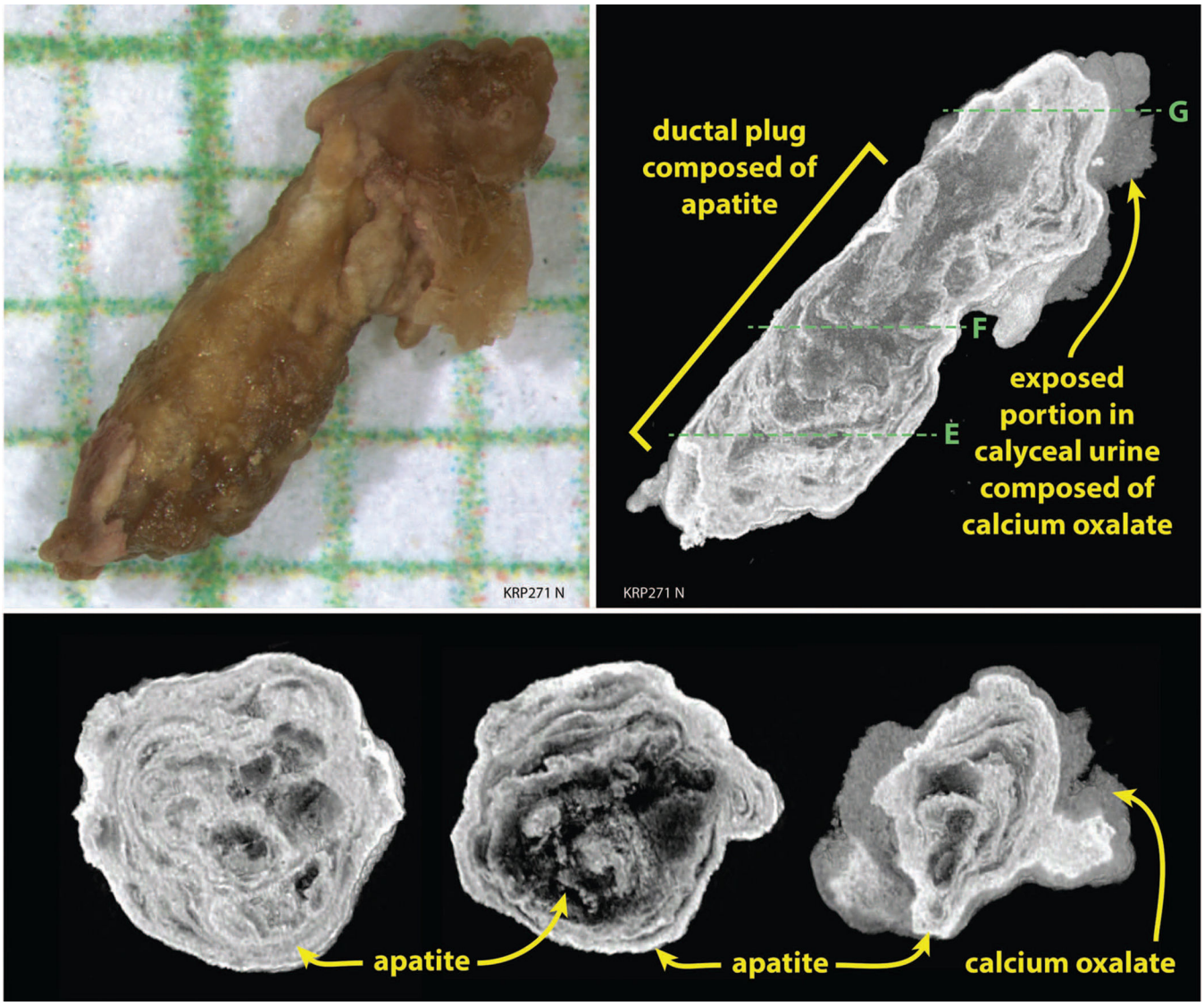

Figure 4. Fine structure of MSK ductal stones, and BD plugs

Panel a shows a ductal stone after being released from a dilated IMCD by a holmium laser and placed on a millimeter grid; arrow marks the region obliterated by the laser used to open the cavity. Panel b is a representative μCT slice through the ductal stone seen in panel a and shows that the interior of the stone consists of apatite (bright white) which appears to have been laid down in concentric rings. The outer portion of the stone is covered by calcium oxalate monohydrate (COM). Volume percentages in this stone are 46% apatite and 54% COM. Panel c is a BD plug with overgrowth that was pulled from an MSK papillum (on millimeter grid). Panel d is a representative μ-CT longitudinal slice through the BD plug and overgrowth seen in panel c; the overgrowth of calcium oxalate was visible on the surface of papillum by endoscopy before removal. Panels e, f, and g are representative μ-CT cross-sections through the BD plug with overgrowth shown in panels c and d to show the change in mineral content and mineralization pattern between the BD plug and its overgrowth. Lines in panel d show the regions of cross sectional views.

Author Manuscript Author Manuscript Author Manuscript Author Manuscript

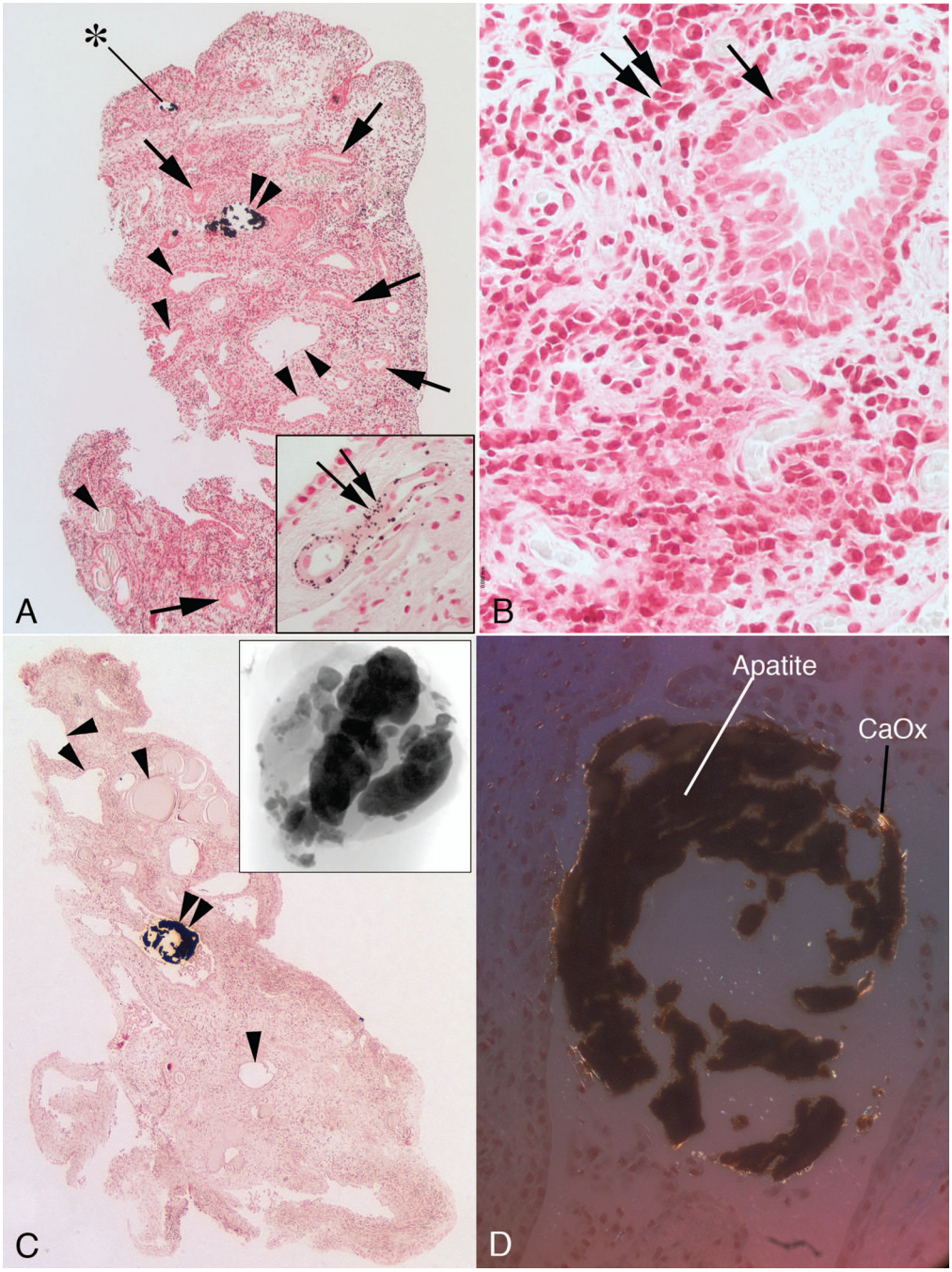

Figure 5. Histologic images of papillary biopsies from MSK patients

The inner medulla of the MSK papilla have unique morphologic characteristics consisting of multilayered lining cells of IMCDs (panels a and b, arrows) and a highly cellular interstitium (panel b, double arrows) whose cells have a primitive fibroblast - like appearance. Typical sites of Randall's plaque (panel a, double arrow in insert) were seen in the basement membrane of the thin loops of Henle. In addition, numerous IMCD were dilated (panels a and c) with some containing mineral (panels a and c, double arrowheads) and others without mineral (panels a and c, arrowheads). The lining cells of the dilated IMCD, though generally

multilayered, varied; some IMCD have a single cell layer. Intraluminal IMCD deposits termed ductal stones were found within dilated tubules (panels a and c, double arrowheads), varied in size (panel c, micro-CT image in insert) and were unattached (floating free) to the lining cells (panels c and d). By polarizing optics the mineral composition of the ductal stones was a mixture of apatite (dark regions) and calcium oxalate (bright regions) (panel d). Only one IMCD plug was found by histopathology (panel a, asterisk) and it was not associated with interstitial fibrosis.

Author Manuscript Author Manuscript Author Manuscript Author Manuscript

Author Manuscript Author Manuscript Author Manuscript Author Manuscript

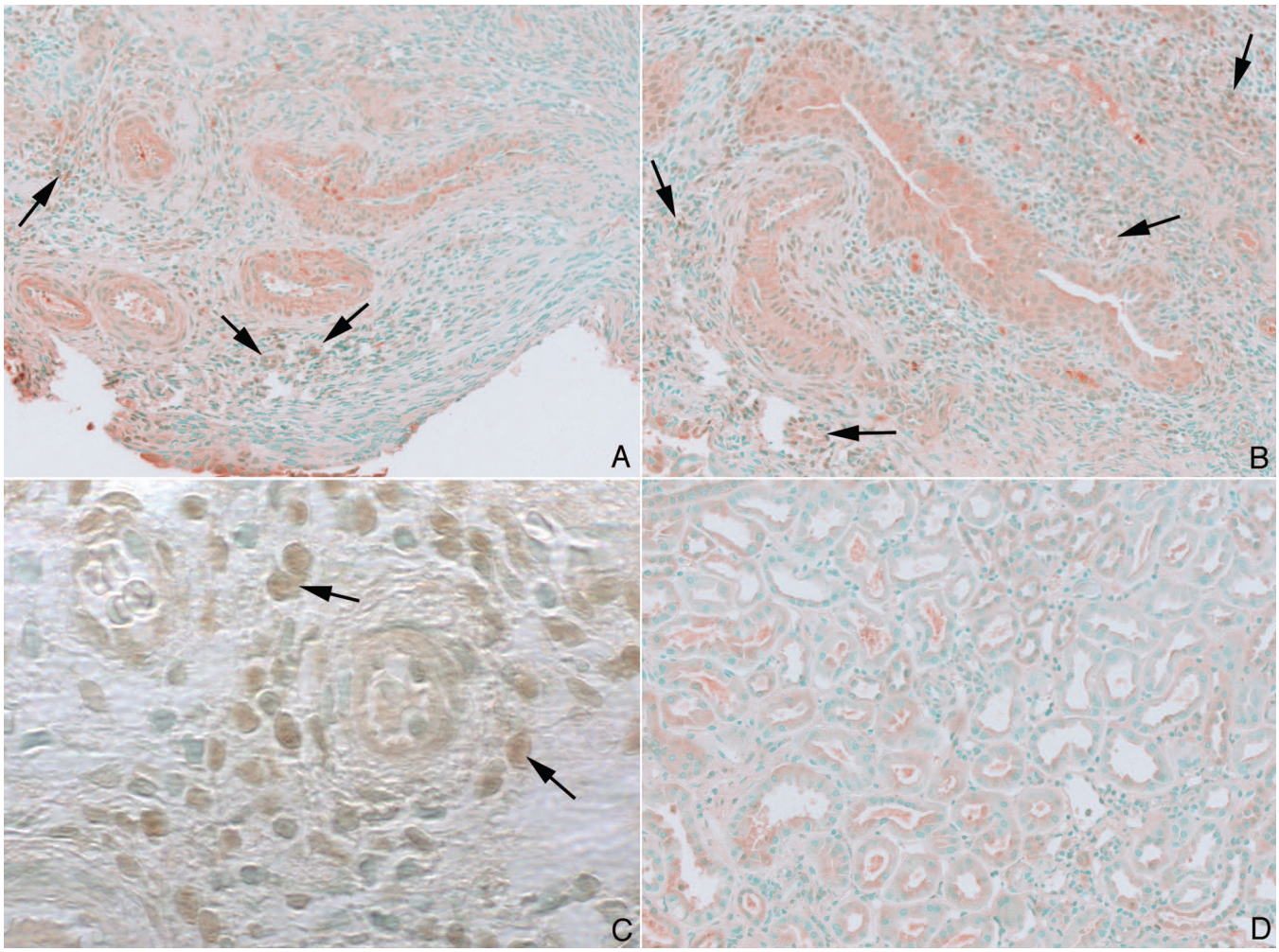

Figure 6. Immuno staining pattern for Runx2 in MSK and ICSF papillary biopsies

Some nuclei of the interstitial cells in papillary sections from MSK patients stained positively for Runx2 (panels a–c, arrows). No staining was seen in the papillary sections from ICSF patients (panel d).

Author Manuscript Author Manuscript Author Manuscript Author Manuscript

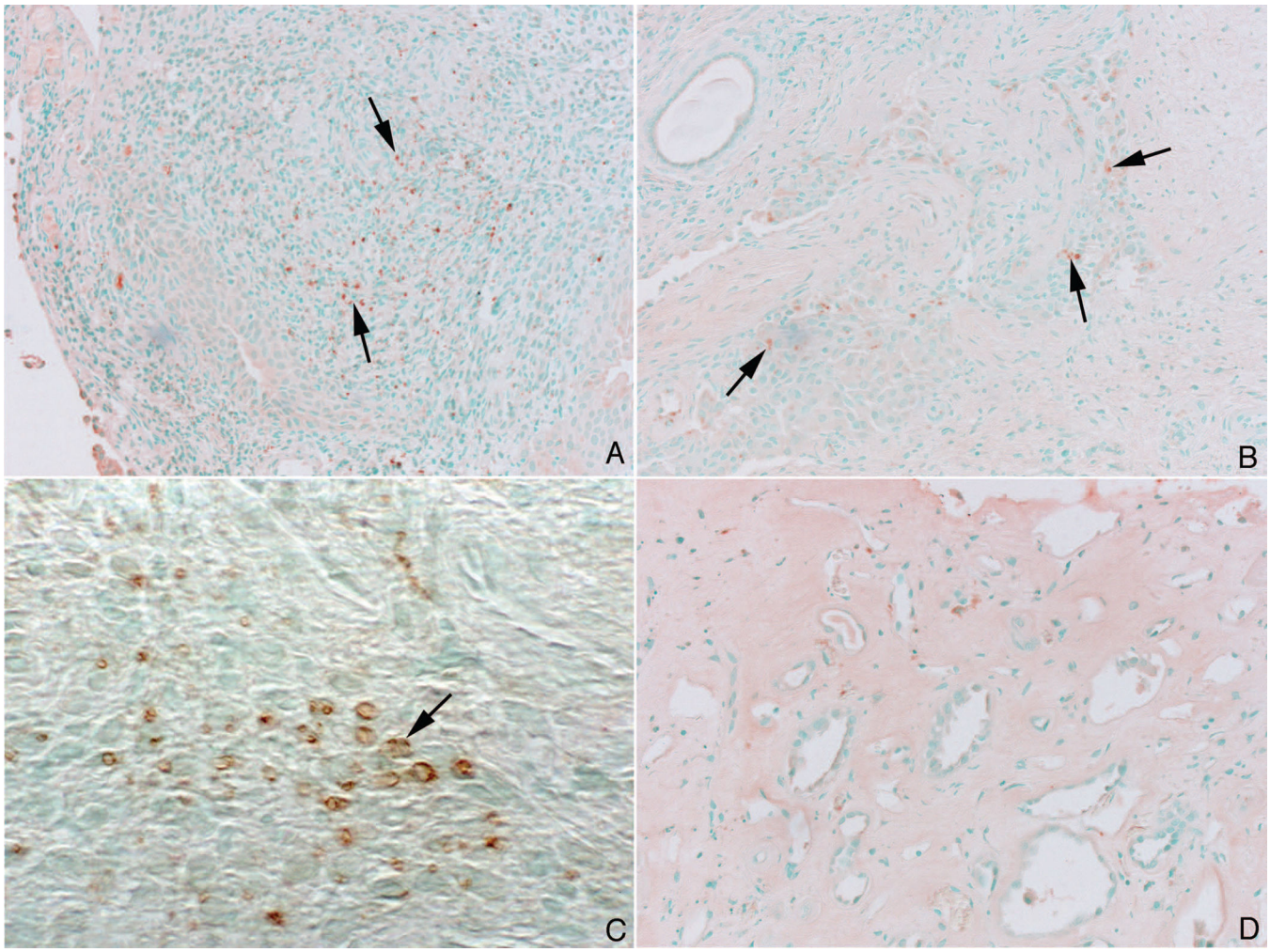

Figure 7. Immuno staining pattern for Osterix in MSK and ICSF papillary biopsies

Like the staining pattern seen for Runx2, some nuclei of the interstitial cells in papillary section from MSK patients stained positively for osterix (panels a–c, arrows). No staining was seen in the papillary sections from ICSF patients (panel d).

Author Manuscript Author Manuscript Author Manuscript Author Manuscript

TABLE 1

CLINICAL CHARACTERISTICS OF MEDULLARY SPONGE KIDNEY STONE FORMERS

Case	Sex	Age first stone	Age at biopsy	Symptomatic stones	Stone location	Hx of UTI	FH of stones	Procedures			Stone analysis (%)			
								ESWL	PNL	URS	#	CaOx	AP	BR
1	M	22	66	> 40	Bilateral	No	Yes	1	0	2	2	99	1	-
2	F	29	41	“multiple”	Unilateral	No	No	1	-	-	1	99	1	-
3	M	19	52	> 100	Bilateral	Yes	No	> 10	0	2	10	41	56	-
4	F	31	43	“multiple”	Bilateral	Yes	Yes	1	0	2	2	-	60	40
5	F	40	43	6	Unilateral	Yes	No	4	0	2	2	100	-	-
6	F	36	36	1	Bilateral	No	Yes	0	0	0	1	100	-	-
7	F	37	42	> 20	Bilateral	Yes	No	1	0	1	4	18	82	-
8	F	18	48	> 100	Bilateral	No	Yes	1	0	0	2	68	28	-
9	M	37	38	3	Bilateral	Yes	Yes	0	0	1	3	37	63	-
10	F	18	60	> 50	Bilateral	Yes	No	8	0	1	1	100	-	-
11	M	18	55	> 100	Bilateral	Yes	No	25	2	9	12	48	19	33
12	F	18	38	> 10	Bilateral	Yes	Yes	2	0	2	5	84	16	-

UTI, urinary tract infection; FH, family history; Procedures, procedures prior to current PNL; ESWL, extracorporeal shock wave lithotripsy; PNL, percutaneous nephrolithotomy; URS, ureteroscopy; Stone analysis #, number of stone analyses from commercial labs available; CaOx, calcium oxalate; AP, apatite; BR, brushite. Stones containing traces of uric acid found in patient 8.

Anat Rec (Hoboken). Author manuscript; available in PMC 2016 May 01.

Author Manuscript Author Manuscript Author Manuscript Author Manuscript

TABLE 2

SERUM AND URINE MEASUREMENTS IN MEDULARY SPONGE KIDNEY STONE FORMERS

Case	SERUM			URINE									
	Creat mg/dl	K mmol/L	HCO3 meq/L	Vol l/day	pH	Calcium mg/d	Oxalate mg/d	Citrate mg/d	Sulfate meq/d	NH4 mmol/d	Ca/Cr mg/gm	SS CaOx	SS CaP
1	1.0	4.0	24	3.16	5.96	275	49	347	51	58	142	5.62	0.63
2	0.6	4.2	24	1.41	5.48	239	28	931	43	31	201	9.22	0.87
3	1.4	3.7	31	3.41	6.55	212	56	285	33	32	94	5.53	0.90
4	0.5	3.2	26	1.29	6.30	229	43	285	35	39	214	12.1	2.30
5	0.7	3.9	27	1.55	6.11	164	24	519	36	36	138	5.19	0.95
6	0.7	4.1	28	1.42	5.95	240	37	685	44	29	184	10.58	1.22
7	0.7	4.4	24	2.80	5.93	149	40	548	17	34	135	4.45	0.22
8	1.0	4.0	24	1.73	6.09	272	33	994	30	23	187	7.51	1.47
9	0.9	4.2	28	2.21	5.92	199	30	255	31	30	93	4.41	0.69
10	1.0	4.5	25	3.72	6.10	231	38	806	26	24	207	3.45	0.35
11	1.2	4.1	24	3.50	6.32	473	62	2370	58	53	199	8.30	1.83
12	-	-	-	1.30	6.30	324	31	536	30	18	252	11.1	3.65
Mean	0.9±0.1	4.0 ± 0.1	26 ± 0.7	2.3±0.2	6.1±0.1	250±18	39±3	641±76	36±2	34±2	170±13	7.3±0.8	1.3±0.3

Data for each patient is the mean of two 24 hour urines done off medications; a single serum was measured for each patient. Values are means and SEM. Creat, creatinine; Vol, volume; NH4, ammonium; Ca, calcium; Cr, creatinine; SS, supersaturation; CaOx, calcium oxalate; CaP, calcium phosphate.

Anat Rec (Hoboken). Author manuscript; available in PMC 2016 May 01.

Author Manuscript Author Manuscript Author Manuscript Author Manuscript

TABLE 3

ANALYSES OF RENAL MINERAL BY MICRO-CT

	Bellini Duct Plugs*				Ductal Stones				Stones on Randall's plaque				Renal pelvis			
Case	**#**	**CaOx%**	**AP%**	**BR%**	**#**	**CaOx%**	**AP%**	**BR%**	**#**	**CaOx%**	**AP%**	**BR%**	**#**	**CaOx%**	**AP%**	**BR%**
1	—	—	—	—	1	90	10	0	1	97	3	0	9	94	6	0
2	—	—	—	—	—	—	—	—	—	—	—	—	9	97	3	0
6	—	—	—	—	20	62	38	0	—	—	—	—	1	82	18	0
7	5	2	98	0	6	10	90	0	—	—	—	—	4	0	100	0
8	1	60	40	0	—	—	—	—	—	—	—	—	9	98	2	0
9	-	-	-	-	1	72	28	0	—	—	—	—	2	74	26	0
10	—	—	—	—	34	80	20	0	1	—	—	—	13	91	9	0
11	—	—	—	—	10	28	25	47	2	41	10	48	3	19	10	71
12	—	—	—	—	10	80	20	0	—	—	—	—	3	73	27	0

*Each of the plugs had an overgrowth that extended into the calyceal urine. The compositions of the overgrowths differed from the composition of the plugs. In patient 7 the overgrowths were composed of 63% CaOx, 37% AP. In patient 8 the overgrowth was composed of 99% CaOx and 1% AP.

Author Manuscript Author Manuscript Author Manuscript Author Manuscript

TABLE 4

PAPILLARY AND CORTICAL PATHOLOGY

Case	Papillary pathology		Glomerular pathology			Cortical pathology		Plaque coverage (% of surface)		
	Ductal stones	IMCD Deposits	Total glomeruli	Mild	Global	Tubular atrophy	Interstitial fibrosis	Kidney	White	Yellow
1	9	2	-	-	-	-	-	L	1.39	0
2	2	0	8	0	0	0	0	R	4.26	0
3	2	0	-	-	-	-	-	L	0.57	0.09
4	13	1	47	0	36	2	1	L	0.67	0
5	1	0	-	-	-	-	-	R	0.16	0
6	1	0	15	0	1	1	1	L R	3.21 2.64	0 0
7	4	1	11	0	0	1	1	L R	1.09 2.06	0.03 0
8	9	0	1	0	1	1	1	L	0.93	0
9	1	0	24	6	4	2	1	L	0.27	0
10	9	1	21	0	9	1	1	L R	0.71 1.02	0.12 0.11
11	3	0	8	0	0	1	1	L	1.80	0.03
12	3	0	19	0	0	1	1	L R	3.60 1.82	0 0.17

Ductal stones, #/mm^3; Deposits, #/mm^3; Fibrosis graded 0–3; Mild/global sclerosis = total number glomeruli; Tubular atrophy graded 0–3; Interstitial fibrosis graded 0–3; plaque coverage,

Anat Rec (Hoboken). Author manuscript; available in PMC 2016 May 01.

Author Manuscript Author Manuscript Author Manuscript Author Manuscript

TABLE 5

CORRESPONDENCE OF COMPOSITION OF MINERAL IN SIX SITES IN MSK STONE FORMERS

Case	Clinical Stones	Renal Pelvis Stones	Ductal Stones	BD Plugs	Overgrowths on Plugs	Stones on Plaque
1	CaOx	CaOx	CaOx	-	-	CaOx
2	CaOx	CaOx	-	-	-	-
3	HA	-	-	-	-	-
4	HA+BR	-	-	-	-	-
5	CaOx	-	-	-	-	-
6	CaOx	CaOx	CaOx	-	-	-
7	HA	HA	HA	HA	CaOx	-
8	CaOx	CaOx	-	CaOx	CaOx	-
9	HA	CaOx	CaOx	-	-	-
10	CaOx	CaOx	CaOx	-	-	-
11	CaOx +BR+HA	BR+ CaOx +HA	BR+ CaOx +HA	-	-	BR+ CaOx +HA
12	CaOx	CaOx	CaOx	-	-	-

A seventh site of mineralization, IMCD plugging, was seen in patient 1; the plug was composed of HA. CaOx, calcium oxalate; HA, apatite; BR, brushite.